Separation Science and Technology
Publication details, including instructions for authors and subscription information:
http://www.informaworld.com/smpp/title~content=t713708471

Comparison of Gravitational SPLITT Fractionation with Gravitational Settling for Separating Micron Size Particles

Nongnuch Tantidanai[a]; Waret Veerasai[a]; Ronald Beckett[b]
[a] Department of Chemistry, Faculty of Science, Mahidol University, Bangkok, Thailand [b] Water Studies Centre, School of Chemistry, Monash University, Clayton, Australia

To cite this Article Tantidanai, Nongnuch , Veerasai, Waret and Beckett, Ronald(2006) 'Comparison of Gravitational SPLITT Fractionation with Gravitational Settling for Separating Micron Size Particles', Separation Science and Technology, 41: 13, 3003 — 3025
To link to this Article: DOI: 10.1080/01496390600786176
URL: http://dx.doi.org/10.1080/01496390600786176

Separation Science and Technology, 41: 3003–3025, 2006

ISSN 0149-6395 print/1520-5754 online
DOI: 10.1080/01496390600786176

Comparison of Gravitational SPLITT Fractionation with Gravitational Settling for Separating Micron Size Particles

Nongnuch Tantidanai and Waret Veerasai
Department of Chemistry, Faculty of Science, Mahidol University, Rama 6 RoadBangkok, Thailand

Ronald Beckett
Water Studies Centre, School of Chemistry, Monash University, Clayton, Australia

Abstract: The performance of gravitational Split-flow thin-channel (GrSPLITT) fractionation has been compared with conventional gravitational settling (GrSettling) method. Two modes of GrSPLITT (full-feed depletion (FFD) mode and transport (TS) mode) were employed. Silica and natural river particles were used to test these techniques. The particles were fractionated at the following cutoff diameters (d_c) 2, 4, 6, 10, 14, and 20 μm. The fractions with diameter $< d_c$ were analyzed for their particle size distribution by both optical or scanning electron microscopy and image analysis. Several parameters were used to objectively compare the efficiency of the methods. Almost all of the tests showed that TS-GrSPLITT had the highest separation efficiency. The ranking of FFD-GrSPLITT and GrSettling were considered to be of equal ranking as the order varied for the different parameters and samples used.

Keywords: SPLITT fractionation, setting method, particles

Received 21 February 2006, Accepted 17 April 2006
Address correspondence to Waret Veerasai, Department of Chemistry, Faculty of Science, Mahidol University, Rama 6 Road, Bangkok, 10400, Thailand. E-mail: scwvr@mohidol.ac.th and Ronald Beckett, Water Studies Centre, School of Chemistry, Monash University, Clayton VIC 3168, Australia. E-mail: ron.beckett@sci.monash.edu.au.

INTRODUCTION

Trace elements in natural water can be present in a number of forms including association with colloidal or suspended particles. The interactions of trace elements with aquatic biota are largely influenced by the forms of the trace elements. Speciation distribution studies have shown that trace element concentrations in soils and sediments vary with the nature of the particles and with particle size (1–8). Thus there is a need for both chemical and physical (size-based) speciation information.

Size-based speciation methods require an efficient particle size fractionation technique. Conventional size separation techniques such as filtration and gravitational settling have been commonly used for fractionating environmental samples, however, both have limitations (Gimbert et al. 2005 EST in press).

Gravitational split-flow thin-channel (GrSPLITT) fractionation is a new binary separation method which can have high resolution and produce rapid continuous separations of micron size particles. GrSPLITT can be operated in two ways; transport (TS) mode and full-feed depletion (FFD) mode. In this work, a comparison of the separation efficiency of gravitational settling and the two modes of GrSPLITT fractionation was investigated.

In an attempt to objectively compare the performance of the three methods several parameters have been used. One aim of the paper is to evaluate the usefulness of these measures of separation efficiency in such comparative studies.

Gravitational Settling

Gravitational settling (GrSettling) is a classical method for particle size separation commonly employed in soil and sediment studies. However, it can have a long separation time, especially for small particle cutoff sizes.

One of the most common procedures using GrSettling is referred to as the pipette method. A particle suspension is added to a cylinder and stirred to obtain homogeneity. At a certain time (t) and depth (x), corresponding to a specified cutoff diameter (d_c), a sample aliquot is removed with a pipette. This fraction contains a representative sample of particles with diameters less than the cutoff ($<d_c$). This method is cheap but for particles <5 μm can be time consuming. Problems with resolution can be encountered due to the difficulty in withdrawing the sample without disturbance.

GrSettling methods are usually based on Stokes law which describes the settling behavior of a single sphere, under gravity, in a fluid of infinite extent. At low Reynolds numbers, the Stokes diameter, which for a spherical particle is its physical diameter, is given by (9)

$$d_c = \sqrt{\frac{18\eta x}{g\Delta\rho t}} \tag{1}$$

where d_c is the cutoff diameter, η is the fluid viscosity, x is the distance a particle settles after time t, g is the gravitational acceleration, and $\Delta\rho$ is the difference in densities of the particle and the fluid.

GrSPLITT Fractionation

A split-flow separation cell is a thin (generally sub-millimeter) rectangular channel in which various physical forces are utilized to drive components across the thin dimension of the channel, as illustrated in Fig. 1. One advantage of thin channels is that the settling distance is small (usually <1 mm) hence the separation is quite rapid. Various fields and gradients have been used as driving forces in SPLITT fractionation, including gravitational and centrifugal sedimentation, diffusive transport, electrical and magnetic fields, and hydrodynamic lift forces (10–12). At the same time liquid flowing lengthwise along the channel causes the sample components to be flushed through. By splitting the outlet flows, the suspended material can be separated into two substreams containing particles of different sizes.

The concepts involved in utilizing gravitational forces in the transport mode and full-feed depletion mode are illustrated in Figs. 1a and 1b respectively. In the transport mode, a suspended sample is introduced into one inlet (*a*'), while a carrier is introduced into the other inlet (*b*') at flow rates several times higher than the sample inlet stream. This procedure initially confines the sample in a

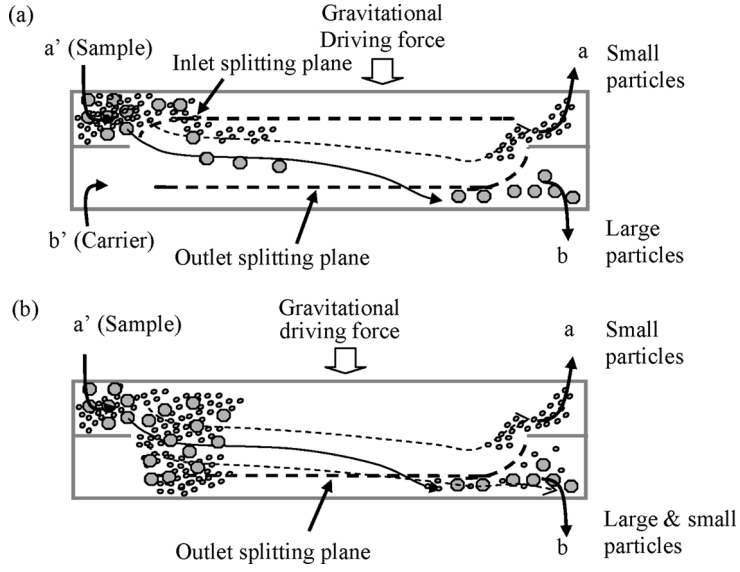

Figure 1. Diagram of (a) transport mode and (b) full-feed depletion mode of GrSPLITT fractionation.

thin zone at the top of the channel, which improves the separation resolution (Fig. 1a). The bold dashed line in Fig. 1a labeled the inlet splitting plane (ISP) defines the plane where the two inlet streams meet and its position depends on the ratio of flow rates. An outlet splitting plane (OSP) is also shown which separates fluid laminar which will eventually exit from either outlet *a* or *b*.

On entering the channel and being concentrated near the upper wall just beyond the end of the inlet splitter, sample components then settle towards the bottom at different velocities. Faster settling components may move past the OSP and exit from outlet *b* as illustrated by the large particles in Fig. 1a. The small particles shown do not reach the OSP during their time in the channel and exit outlet *a*. Thus a binary separation of the two components is achieved. In a sample with a continuous size distribution the largest particle diameter that cannot move past the OSP is the cutoff diameter (d_c). In this case the fraction with diameter $<d_c$ is obtained from outlet *a* and the fraction $>d_c$ is obtained from outlet *b*.

For the transport mode the cutoff diameter is calculated from Equation (2) (3). Where $\dot{V}'_a$ is the sample inlet flow rate, $\dot{V}_{a'}$ is the upper outlet flow rate, *b* is breadth of the GrSPLITT channel, and *L* is distance between the end of the inlet and outlet splitters in the channel.

$$d_c = \sqrt{\frac{18\eta(\dot{V}_a - \dot{V}_{a'})}{bLg\Delta\rho}} \tag{2}$$

In the full-feed depletion mode there is no carrier inlet and hence no ISP. The sample spreads across the entire channel thickness immediately after entering the channel. At a suitable time the sample to be driven to each side of the outlet splitting plane (OSP) then separation will occurr. All particles greater than a certain cutoff diameter settle in the OSP and exit via outlet *b* there will always be some smaller particles smaller than the cutoff diameter present below the OSP. This causes no ISP to control the settling point for all particles in the channel. The cutoff diameter is calculated from Equation (3) (3).

$$d_c = \sqrt{\frac{18\eta(\dot{V}_{a'} - \dot{V}_b)}{bLg\Delta\rho}} \tag{3}$$

where $\dot{V}_b$ is the lower outlet flow rate.

EXPERIMENTAL

Preparation of Suspensions

Silica particles (nominally 1–10 μm) from Kromachem Ltd, Watford, UK were suspended in deionized water only at a solids concentration of 0.2% w/v. For all samples, the pH was kept constant at 6.

Chaopraya River water was collected from the surface on June 22nd, 2003, at 2.30 p.m. at the Samlae raw water pumping station of Metropolitan Waterworks Authority (MWA) in Pathum Thani, Thailand. The Samlae station is the first point that takes water from the Chaopraya River into the MWA's East Canal. It is located in Samlae, Pathum Thani, which is 41 kilometers away from Bangkok, and 90 kilometers from the Gulf of Thailand. Twenty liters were sequentially filtered through 48 μm and 22 μm nylon sieves to remove debris, sand, and coarse silt. The filtrate (i.e. fraction <22 μm) was concentrated (1:20) by centrifugation at 3000 rpm for 20 min corresponding to a calculated cutoff diameter of 0.45 μm. The sample fraction $0.45 < d < 22$ μm was stored at 4°C.

Gravitational Settling Method

A suspended sample was put in a 500 mL measuring cylinder and thoroughly mixed using a stirring rod. After a certain settling time, a pipette was used to remove a 10 mL aliquot at a specified depth. This fraction ($<d_c$) should contain particles smaller than the desired cutoff diameter calculated using Equation (1). The fractions were stored in a refrigerator at 4°C.

GrSPLITT Apparatus

A GrSPLITT channel was obtained from Postnova Analytics (Salt Lake City, UT, USA). The working dimensions of the channel were a distance between splitting planes of 10 cm, breadth 1.5 cm, and thickness 0.061 cm. The channel contained a stainless steel splitter which was sandwiched between two Teflon spacers. All of these components were held together firmly by two Lucite blocks (1–4).

Two peristaltic pumps from MasterFlex (L/S Model 7523-25) provided the independent flows to inlets a' and b' in a TS-GrSPLITT experiment or one in the case of a FFD-GrSPLITT experiment. A peristaltic pump (Gilson Minipuls, Middleton, WI) controlled the outlet flow a. The flow rates were measured with a burette or electronic balance and stop watch. All pumps were adjusted to the required flow rates using water before the suspended sample suspension was introduced continuously into the GrSPLITT channel through inlet a'.

Optical and Scanning Electron Microscopes with Image Analysis

An optical microscope with image analysis was used to count and measure the sizes of the silica. Scanning the electron microscope with image analysis was used to count and measure the sizes of the Chaopraya River suspended particles. Between 500–1000 particles were measured on each photomicrograph and each photomicrograph was processed three times using the image analysis program.

A hemacytometer counting chamber is an etched glass chamber with raised sides that holds a quartz cover slip exactly 0.1 mm above the

chamber with a total surface area of 9 mm^2. It was filled with the silica suspension and covered with a glass slide. Optical photomicrographs of the settled silica particles and grid were obtained using an OLYMPUS CH2 OM equipped with a PULNiX TM-6CN digital camera, full field 768W × 512H pixels. The optical photomicrographs were used to measure the number and sizes of the silica particles using Optimas 6.5 Copyright© 1999 Media Cybernetics, L.P. image analysis software. This generated a list of the size of each particle on the photo. Excel was used to sort the list in order of increasing size and to generate the number of particles in ranges 1–3 μm, 3–5 μm, and 31–33 μm.

The SEM photomicrographs of Chaopraya River suspended particles were obtained using a JOEL JSM-840A SEM. This instrument was upgraded by the addition of an Oxford Instruments ISIS 300 energy dispersive analytical system with a high-purity Germanium detector, a backscatter electron detector, Deben stage automation, and a Semafore digital image acquisition. Known volumes of the original sample and separated fractions were filtered through 0.2 μm pore size polycarbonate membranes (Nucleopore™). The air dried samples were vacuum coated with Au. The SEM photomicrographs were used to measure the number and size of the Chaopraya River suspended particles using the Optimas 6.5 image analysis software.

RESULTS AND DISCUSSION

Model silica and natural Chaopraya River samples were used to compare the separation efficiency of the three methods. The $<d_c$ fraction for each sample was collected after GrSettling (pipette fraction), FFD-GrSPLITT (fraction *a*), and TS-GrSPLITT (fraction *a*) for the following cutoff diameters 2, 4, 6, 10, 14, and 20 μm. Particle size distributions were measured using OM or SEM and image analysis. The precision of the counts in each size bin was estimated from the triplicate measurement of the photos and the relative standard deviation was usually in the range 1–2%. Various parameters, derived from the number and mass based distribution of the original samples and the $<d_i$ fractions collected at various cutoffs for the two samples, were used to compare the separation efficiency of the three methods where d_i is the mid range diameter ($d_i = 2$ μm for the fraction range 1–3 μm, $d_i = 4$ μm for the fraction range 3–5 μm, $d_i = 6$ μm for the fraction range of 5–7 μm). These comparisons are discussed below.

Optical and SEM Photomicrographs of Separated Fractions

Optical photomicrographs of the original silica and the fractions collected from some of the size cutoffs made using FFD-GrSPLITT are shown in

Fig. 2. Good separation appears to have been achieved for three spherical particles with most of the particles being sorted into the appropriate fraction. However, it is obvious that some of the particles have diameters outside the expected range.

SEM photomicrographs of the <6 μm and >6 μm Chaopraya River fractions obtained using GrSettling, FFD-GrSPLITT, and TS-GrSPLITT is given in Fig. 3. The sample is rather heterogeneous in shape and appears to contain many platey particles. Some of the particles have a diameter outside

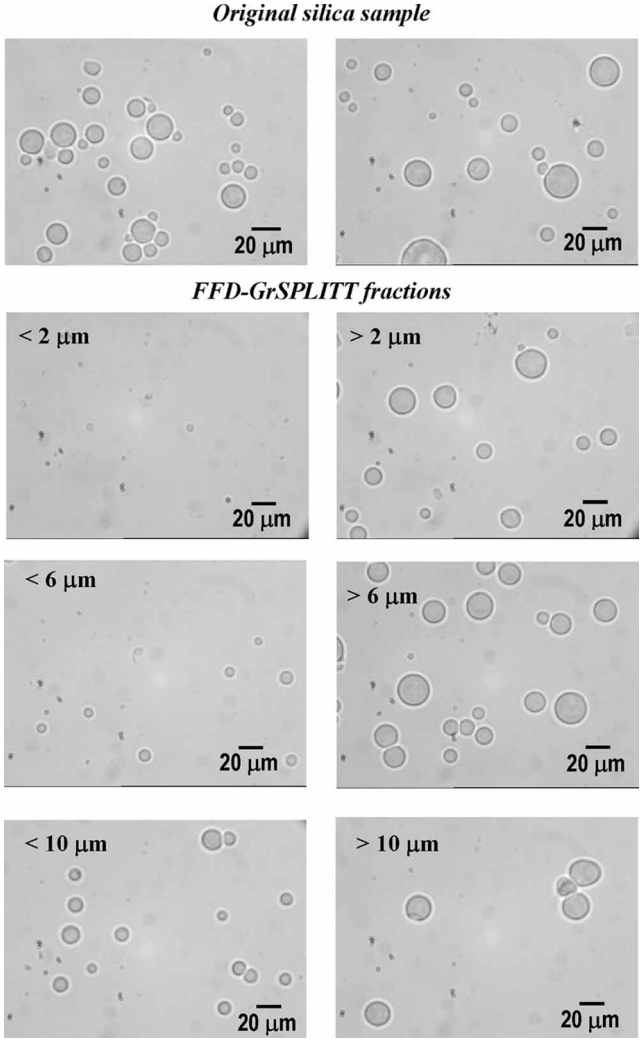

Figure 2. Photomicrographs of silica particles before and after size separation using FFD-GrSPLITT fractionation. The cutoff diameters are 2, 6, 10, and 20 μm.

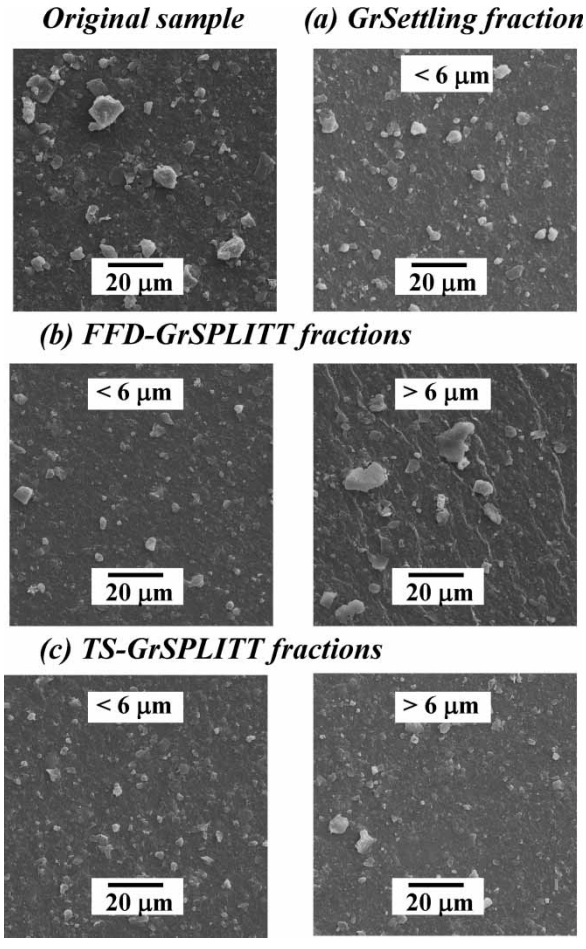

Figure 3. Comparison of electron photomicrographs of Chaopraya River (Thailand) suspended particles separated using three different methods (a) GrSettling, (b) FFD-GrSPLITT, and (c) TS-GrSPLITT. The cutoff diameters were all 6 μm.

the expected range. The separation process here is complicated by variations in particle shape and perhaps density. More objective quantitative means are required to compare the efficiency of the fractionation methods in detail.

Size Distributions of Separated Fractions

The particle number-based differential size distributions were measured directly from the photomicrographs by image analysis. These distributions are plotted as the number of particles in each 2 μm wide bin versus the

mid-range diameter (μm). The distributions for the silica sample and the <2 μm, <6 μm, and <10 μm fractions are given in Fig. 4. The size distributions for the $<d_c$ fractions indicate an increased removal of particles from the original sample as the cutoff diameter decreases as expected. The

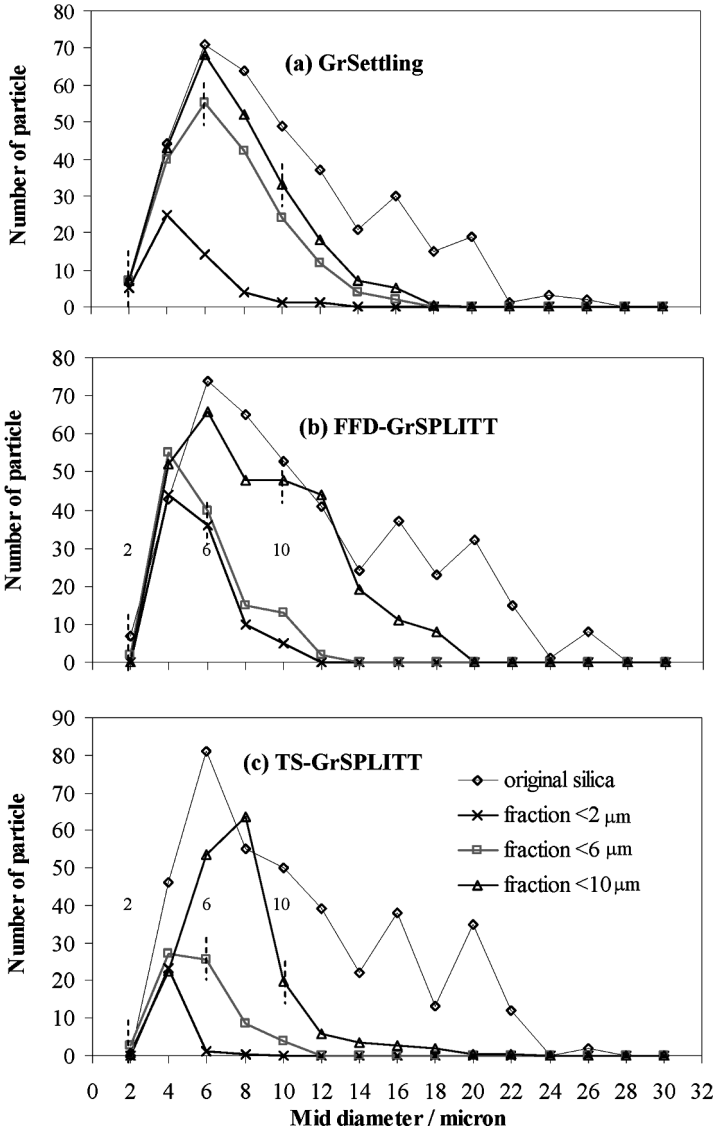

Figure 4. Differential number-based particle size distribution curves of the silica sample and fraction less than 2, 6, and 10 μm using three methods: (a) GrSettling, (b) FFD-GrSPLITT, and (c) TS-GrSPLITT.

theoretical cutoff diameter for each fraction is shown as a short vertical dashed line. Clearly some particles with diameter $>d_c$ are removed from the fractions and not all particles with size $<d_c$ are removed.

The volume (or mass) based size distributions were computed from the number data. For the Chaopraya River sample the vast majority of particles are less than 4 μm. However, the volume-based distributions, which are shown in Fig. 5, indicate a significant mass of particles up to about 14 μm. Again these distributions indicate a reasonable separation was achieved but quantitative measures are required for a detailed assessment of the efficiency of each method. Several such approaches are outlined below.

Percent Removal of Particles after Fractionation

The differential distributions of the original sample and the fractions at each cutoff (d_c) were used to compute the percent number of particles removed in each diameter range (specified by the mid-range diameter d_i). The percentage of particles in the $<d_c$ fraction removed from the total sample in each size range were calculated from

$$\%R_{d_i}^N = \frac{(N_{d_i}^s - N_{d_i}^{<d_c})}{N_{d_i}^s} \times 100 \tag{4}$$

where $N_{d_i}^s$ is the number of particles in the d_i size range for the original sample and $N_{d_i}^{<d_c}$ is the number of particles in the same size range in the $<d_c$ separated fraction.

Thus the percentage number removal ($\%R_{d_i}^N$) measures the difference between the number of particles in the size fractions before and after the size separation. These values were then converted to cumulative percent removals which give the number of particles removed up to fraction d_i

$$Cumulative\ \%R_{d_i}^N = \sum_{d_i=1}^{d_i} \%R_{d_i}^N \tag{5}$$

Plots of cumulative $\%R_{d_i}^N$ versus d_i for the silica and Chaopraya River sample were made as shown in Figs. 6 and 7 respectively. Ideally the plots should increase abruptly from 0% removal to 100% removal at the cutoff diameter d_c set for the separation. Although the increases do occur over a range of diameters, the plots do indicate that reasonable separations were achieved.

The slope of the cumulative percent removal distribution curves should ideally be infinity at the cutoff diameter. In practice the higher the slope of the curve, the greater the resolution of the separation.

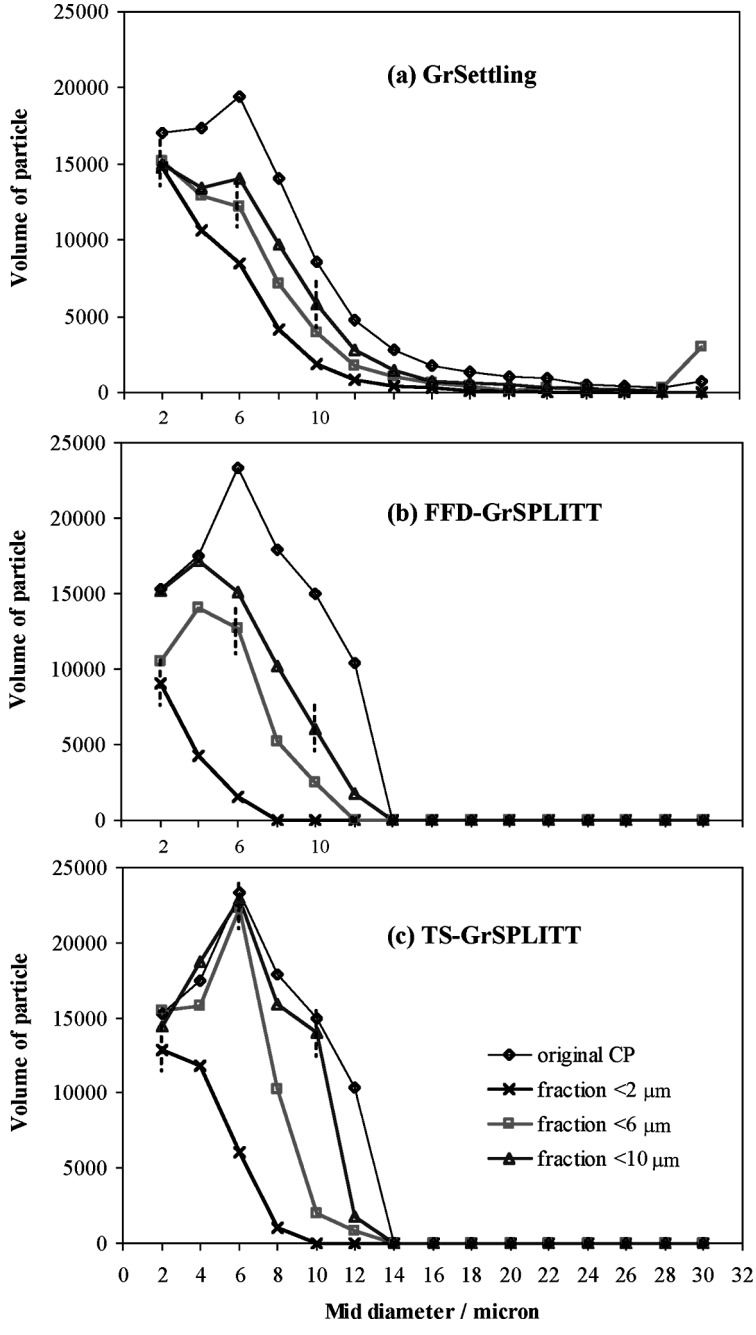

Figure 5. Differential volume-based particle size distribution curves of Chaopraya River suspended particles and fraction less than 2, 6, and 10 μm using three methods: (a) GrSettling, (b) FFD-GrSPLITT, and (c) TS-GrSPLITT.

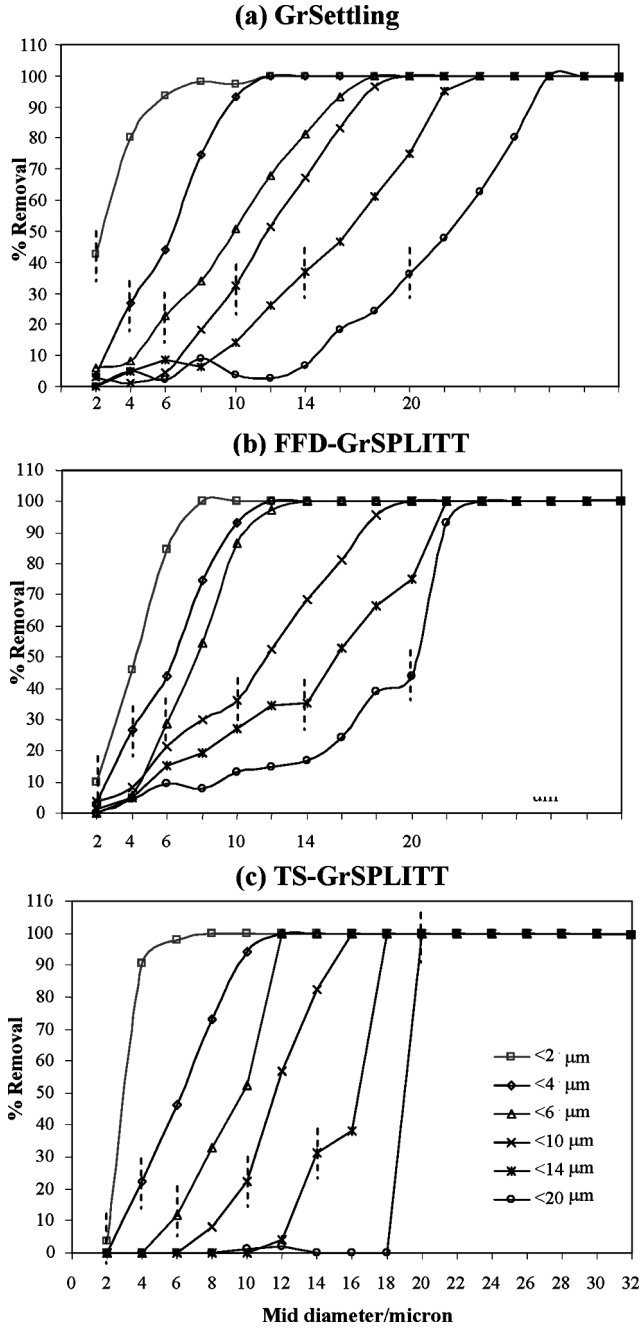

Figure 6. Percentage removal curves of silica particles in following cutoff sizes: 2, 4, 6, 10, 14, and 20 µm using three methods (a) GrSettling, (b) FFD-GrSPLITT, and (c) TS-GrSPLITT. The vertical dashed line indicates the cutoff diameter for each fraction.

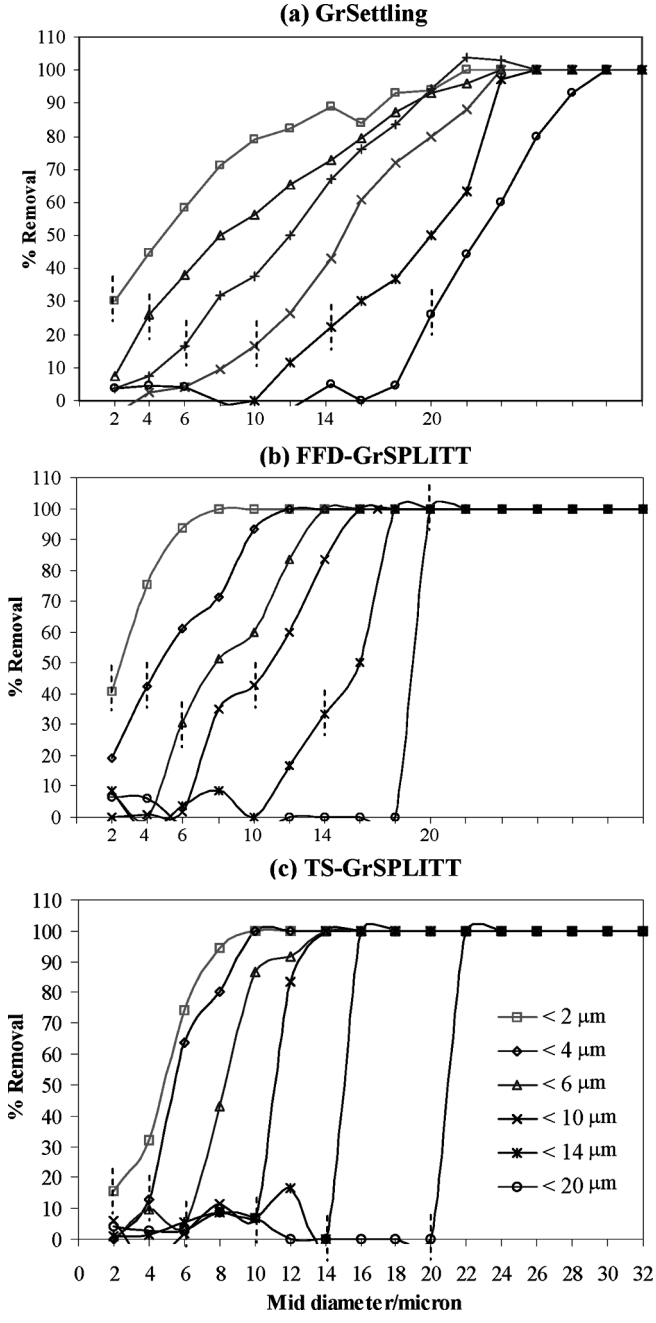

Figure 7. Percent removal curves of the Chaopraya River (Thailand) suspended particles separated using (a) GrSettling, (b) FFD-GrSPLITT, and (c) TS-GrSPLITT for the diameters cutoff 2, 4, 6, 10, 14, and 20 μm.

From the cumulative the $\%R_{d_i}^N$ plots we have calculated some parameters which can be used as a measure of the efficiency of the separations. They are

1. the diameter where 50% of the particles are removed, which should correspond to the calculated value of d_c,
2. the range of diameters where 20%–80% of the particles are removed and
3. the gradient of the best fit line over the range where 10–90% of the particles are removed.

These parameters are listed in Tables 1 and 2 for the silica and Chaopraya River sample respectively.

For each size fraction the three separation methods were ranked 1, 2, or 3 according to the value of the parameter under consideration. Then for each separation method the rank for each of the six fractions of the sample were summed to give the total ranking points for that parameter and technique. The total ranking points for a parameter with a given method will thus fall in the range 6–18 with the lower ranking points allocated indicating the better separation efficiency. The results for both samples show that TS-GrSPLITT has the lowest ranking points based on the diameter range and gradient of the cumulative percent removal category. However, the cutoff diameter category would indicate about equal ranking of the two SPLITT techniques. The results of the ranking scores are discussed in more detail in the section below on comparison of the separation methods.

Percent Error in the Fractionation

A parameter called the percent error was designed which attempts to objectively estimate the efficiency of the separation. This makes use of both the differential number and mass distributions of the original sample and the $<d_c$ fractions separated by the three techniques. For an ideal binary separation no particles should be removed in the size range $<d_c$ and all particles $>d_c$ should be removed. However, in a real separation there will be some error as reflected by the amount of sample removed in the $<d_c$ range and the amount still present in the $>d_c$ range. Thus a percent error can be calculated which is the average of these two errors expressed as a percentage of the amount present in the original sample in each size range. This error can be calculated either from the differential number-based distributions or from the differential volume (or mass)-based size distributions.

A difficulty is encountered in this consideration. In number distributions there is a natural bias towards the smaller particle size end of the distribution so that samples usually contain a large number of particles in the lower size fractions. Hence, appreciable errors often result in subtracting the separated fraction counts from the total sample particle numbers at the lower end of the distribution of the original sample. Conversely small numbers of very

Table 1. The efficiency of GrSettling, FFD-GrSPLITT and TS-GrSPLITT separations using parameters derived from the percent removal of particle number distribution curves for the silica sample given in Fig. 3. Theoretical and estimated (from 50% removal) cutoff diameters, diameter ranges for 20–80% removal, and gradients over the range where 10–90% removal occurs are tabulated

	Cutoff diameter (μm)				Diameter range (μm) for 20–80% removal		Gradient at 10–90% removal	
Method	Theoretical value	Estimated from 50% removal	Deviation	Rank		Rank		Rank
GrSettling	<2	2.4	0.4	1	0.9 − 4.0 = 3.1	2	18.8	2
	<4	6.6	2.6	3	3.4 − 8.4 = 5.0	2	12.6	2
	<6	9.9	3.9	3	5.6 − 13.9 = 8.3	3	7.3	3
	<10	11.7	1.7	2	8.1 − 15.6 = 7.5	2	8.0	2
	<14	16.4	2.4	2	10.9 − 20.4 = 9.5	2	6.0	2
	<20	22.3	2.3	3	16.3 − 26.0 = 9.7	3	6.2	2
Total ranking points				14		14		13
FFD mode of GrSPLITT	<2	4.1	2.1	3	2.5 − 5.8 = 3.3	3	18.6	3
	<4	6.5	2.5	2	3.4 − 8.5 = 5.1	3	11.5	1
	<6	7.6	1.6	1	5.3 − 9.5 = 4.2	1	14.4	1
	<10	11.7	1.7	2	5.7 − 15.9 = 10.2	3	6.2	3
	<14	15.6	2.6	1	8.1 − 20.4 = 12.3	3	4.3	3
	<20	20.3	0.3	1	15.0 − 21.6 = 6.6	2	3.3	3
Total ranking points				10		15		14

(*continued*)

Table 1. Continued

Method	Cutoff diameter (μm)				Diameter range (μm) for 20–80% removal		Gradient at 10–90% removal	
	Theoretical value	Estimated from 50% removal	Deviation	Rank		Rank		Rank
TS mode of GrSPLITT	<2	2.9	0.9	2	2.4 − 3.7 = 1.3	1	43.3	1
	<4	6.3	2.3	1	3.9 − 8.6 = 4.7	1	12.6	2
	<6	9.8	3.8	2	6.9 − 11.1 = 4.2	1	10.2	2
	<10	11.6	1.6	1	9.7 − 13.9 = 4.2	1	14.9	1
	<14	16.4	2.4	2	13.1 − 17.4 = 4.3	1	8.5	1
	<20	19.0	− 1.0	2	18.4 − 19.4 = 1.0	1	50.0	1
Total ranking points				10		6		8

Table 2. The efficiency of GrSettling, FFD-GrSPLITT and TS-GrSPLITT separations using parameters derived from the percent removal of particle number distribution curves for the Chaopraya River sample given in Fig. 3. Theoretical and estimated (from 50% removal) cutoff diameters, diameter ranges for 20–80% removal, and gradients over the range where 10–90% removal occurs are tabulated

	Cutoff diameter (μm)				Diameter range (μm) for 20–80% removal		Gradient at 10–90% removal	
Method	Theoretical value	Estimated from 50% removal	Deviation	Rank		Rank		Rank
GrSettling	<2	4.7	2.7	2	6.0 − 10.1 = 4.1	3	4.1	3
	<4	7.9	3.9	3	3.4 − 15.9 = 12.5	3	3.0	3
	<6	11.9	5.9	3	6.4 − 16.7 = 10.3	3	3.3	3
	<10	14.9	4.9	3	10.6 − 19.7 = 9.1	3	6.2	3
	<14	19.9	5.9	3	13.6 − 22.9 = 9.3	3	4.9	2
	<20	22.6	2.6	3	25.8 − 29.3 = 3.5	3	7.2	3
Total ranking points				17		18		17
FFD mode of GrSPLITT	<2	2.5	0.5	1	0.8 − 4.3 = 3.5	1	13.2	2
	<4	4.7	0.7	1	2.2 − 8.7 = 6.5	2	8.8	2
	<6	7.9	1.9	1	5.2 − 11.7 = 6.5	2	8.3	2
	<10	10.9	0.9	1	7.1 − 13.5 = 6.4	2	8.0	2
	<14	16.0	2.0	2	12.3 − 17.1 = 4.8	2	8.3	3
	<20	18.9	−1.1	2	18.5 − 19.5 = 1.0	1	50.0	1
Total ranking points				8		10		12

(*continued*)

Table 2. Continued

Method	Cutoff diameter (μm)				Diameter range (μm) for 20–80% removal		Gradient at 10–90% removal	
	Theoretical value	Estimated from 50% removal	Deviation	Rank		Rank		Rank
TS mode of GrSPLITT	<2	4.7	2.7	2	2.6 − 6.4 = 3.8	2	14.6	1
	<4	5.3	1.3	2	4.4 − 7.7 = 3.3	1	16.7	1
	<6	8.3	2.3	2	6.9 − 9.5 = 2.6	1	12.2	1
	<10	11.1	1.1	2	10.4 − 11.8 = 1.4	1	17.9	1
	<14	15.0	1.0	1	14.4 − 15.5 = 1.1	1	50.0	1
	<20	20.9	0.9	1	20.4 − 21.6 = 1.2	2	50.0	1
Total ranking points				10		8		6

large particles contribute disproportionately to the particle mass resulting in unreliable values of the mass of particles present in the upper size range of the $>d_c$ fractionated sample. In calculating these errors we found a large variability in the number based error for the $<d_c$ fractions and in the mass based error for the $>d_c$ fractions. Thus in estimating the overall error in a fractionation we chose to use the percent mass of material removed from the original sample for the size range $<d_c$ and the percent number of particles remaining in the separated fraction for the size range $>d_c$. These quantities are calculated as follows:

For the $<d_c$ size range:

$$\%\ mass\ removal\ (<d_c) = \left[\frac{M_{<d_c}^{Total} - M_{<d_c}^{Fraction}}{M_{<d_c}^{Total}}\right] \times 100 \qquad (6)$$

where $M_{<d_c}^{Total}$ is the mass of particles in the total sample before separation in the diameter range $<d_c$, and $M_{<d_c}^{Fraction}$ is the mass of particles in the $<d_c$ fraction after separation in the diameter range $<d_c$.

For the $>d_c$ sizes range:

$$\%\ number\ present\ (>d_c) = \left[\frac{N_{>d_c}^{Fraction}}{N_{>d_c}^{Total}}\right] \times 100 \qquad (7)$$

where $N_{>d_c}^{Fraction}$ is the number of particles in fraction $<d_c$ after separation in the diameter range $>d_c$, and $N_{>d_c}^{Total}$ is the number of particles in the total sample before separation in the diameter range $>d_c$.

The total error in the fractionation is given by the average of these two percent error quantities.

$$\%\ Error = \frac{\%\ mass\ removed\ (<d_c) + \%\ number\ present\ (>d_c)}{2} \qquad (8)$$

The percent errors for the three methods with the silica sample are shown in Table 3. The number in brackets is the standard deviation for the three sets of image analysis data taken from the photographs. The lower the percent error, the greater the separation efficiency of the method. Thus TS-GrSPLITT fractionation was by far the most efficient method with less than 5.3% error for all cutoffs with a mean of 2.3% error. The order of separation efficiency found from the data in Table 3 was TS-GrSPLITT $\gg$ FFD-GrSPLITT $>$ GrSettling.

The percent errors and the mean percent error for the three methods with the Chaopraya River suspended particles are shown in Table 4. For this sample the order is different with TS-GrSPLITT (14.5% mean error) followed by Gravitational settling (18.9% mean error) and FFD-GrSPLITT (26.9% mean error).

Table 3. Percent error of spherical silica particles separated using three methods: (1) gravitational settling, (2) full-feed depletion (FFD) mode and (3) transport (TS) mode of GrSPLITT fractionation techniques

	Percent error (n = 3)					
		GrSPLITT				
		FFD mode			TS mode	
d_c (μm)	GrSettling	Rank		Rank		Rank
2	16.2 ± 1.8	2	20.6 ± 1.6	3	2.1 ± 1.0	1
4	30.1 ± 1.0	2.5	30.1 ± 1.5	2.5	1.4 ± 1.5	1
6	39.0 ± 0.6	3	18.0 ± 0.9	2	5.3 ± 0.6	1
10	24.4 ± 0.4	2	28.8 ± 1.0	3	3.3 ± 1.0	1
14	30.6 ± 1.5	2.5	30.5 ± 1.1	2.5	0.6 ± 0.3	1
20	36.2 ± 0.8	3	17.0 ± 1.0	2	1.1 ± 0.5	1
Mean	29.4 ± 1.0		24.2 ± 1.2		2.3 ± 0.8	
Total rank		15		15		6

Comparison of the Separation Methods

The objectives of this study were twofold; first, to compare the separation efficiency of three different techniques and secondly, to test several different approaches for quantitatively estimating the separation efficiency. Two

Table 4. Percent error of Chaopraya River (Thailand) suspended particles separated using three methods: (1) gravitational settling, (2) full-feed depletion (FFD) mode and (3) transport (TS) mode gravitational SPLITT techniques

	Percent error (n = 3)					
		GrSPLITT				
		FFD mode			TS mode	
d_c (μm)	GrSettling	Rank		Rank		Rank
2	39.0 ± 1.8	3	28.7 ± 1.8	1	32.3 ± 1.5	2
4	12.2 ± 1.4	2.5	13.8 ± 1.5	2.5	6.9 ± 1.9	1
6	16.5 ± 1.1	3	14.0 ± 1.3	2	11.0 ± 1.4	1
10	6.8 ± 1.3	2.5	11.2 ± 1.2	3	5.0 ± 1.7	2.5
14	15.6 ± 1.1	2.5	14.2 ± 1.0	2.5	3.0 ± 0.5	1
20	13.0 ± 1.1	2.5	11.1 ± 1.3	2.5	5.8 ± 1.2	1
Mean	17.2 ± 1.3		15.5 ± 1.4		10.7 ± 1.4	
Total rank		16		13.5		8.5

Table 5. Total ranking point of silica for gravitational settling, full-feed depletion (FFD) mode and transport (TS) mode gravitational SPLITT techniques obtained for theoretical and estimated (from 50% removal) cutoff diameters, diameter ranges for 20–80% removal, and gradients over the range where 10–90% removal occurs are tabulated

	Total ranking point				
Parameter	Cutoff diameter	Diameter range for 20–80% removal	Gradient at 10–90% removal	%Error measure	Overall rank
Method					
GrSettling	14	14	13	15	56
FFD-GrSPLITT	10	15	14	15	54
TS-GrSPLITT	10	6	8	6	30

different samples were employed; a spherical silica and a more heterogeneous river water suspended particulate matter.

In order to compare the methods a ranking point scheme was introduced as outlined in the section above on percent removal. The ranking points for each method obtained for each parameter are tabulated in Tables 5 and 6 for the silica and the Chaopraya River samples respectively. The ranking points for each parameter were also summed to give an overall ranking point for each separation method having a possible range of 24–72.

The lower the ranking points the better the separation achieved for that sample. The results for the silica sample are given in Table 5. TS-GrSPLITT was the best of the methods with 30 overall ranking points.

Table 6. Total ranking point of Chaopraya River sample for gravitational settling, full-feed depletion (FFD) mode and transport (TS) mode gravitational SPLITT techniques obtained for theoretical and estimated (from 50% removal) cutoff diameters, diameter ranges for 20–80% removal, and gradients over the range where 10–90% removal occurs are tabulated

	Total ranking point				
Parameter	Cutoff diameter	Diameter range for 20–80% removal	Gradient at 10–90% removal	%Error measure	Overall rank
Method					
GrSettling	17	18	17	16	68
FFD-GrSPLITT	8	10	12	13.5	43.5
TS-GrSPLITT	10	8	6	8.5	32.5

FFD-GrSPLITT on 54 overall ranking points out of a maximum of 72 and GrSettling with 56 overall ranking points performed about the same. The order of the separation efficiency for the silica separation was TS-GrSPLITT > FFD-GrSPLITT ≅ GrSettling.

Data for the Chaopraya River sample is given in Table 6. In this case the ranking order of the techniques was slightly different with TS-GrSPLITT > FFD-GrSPLITT > GrSettling. It should be noted that not all parameters yielded the same order of efficiency for each fraction and our general conclusion is based on the overall ranking points achieved.

It was found beneficial to use several different parameters in comparing the methods, as the reliance on only one parameter could lead to different conclusions. Indeed the cutoff diameter parameter does give a slightly different order for the separation efficiency TS-GrSPLITT ≅ FFD-GrSPLITT > GrSettling using both samples. It is not significant that there was a slight difference between the rankings obtained with the two samples. The silica results indicated that FFD-GrSPLITT performed about the same as GrSettling where as the Chaopraya River sample showed FFD-GrSPLITT to be slightly better. It is feasible that the particle shape was responsible for this discrepancy.

CONCLUSIONS

Gravitational SPLITT fractionation is a fairly new continuous size separation method that showed the higher separation efficiency than conventional batch gravitational settling methods. For the two modes of GrSPLITT, the transport mode showed a higher separation performance than the full-feed depletion mode. However, the FFD mode has the important advantage that no dilution of the sample is necessary.

ACKNOWLEDGEMENT

The authors thank the PERCH scheme in Thailand for the financial support.

REFERENCES

1. Blo, G., Contado, C., Grandi, D., Fagioli, F., and Dondi, F. (2002) Dimensional and elemental characterization of suspended particulate matter in natural waters: quantitative aspects in the integrated ultrafiltration, splitt-flow thin cell and inductively coupled plasma-atomic emission spectrometry approach. *Anal. Chim. Acta*, 470 (2): 253–262.
2. Camerani, M.C., Steenari, B.-M., Sharma, R., and Beckett, R. (2002) Cd speciation in biomass fly ash particles after size separation by centrifugal SPLITT*1. *Fuel.*, 81 (13): 1739–1753.

3. Contado, C., Dondi, F., Beckett, R., and Giddings, J.C. (1997) Separation of particulate environmental samples by SPLITT fractionation using different operating modes. *Anal. Chim. Acta*, 345 (1–3): 99–110.
4. Crossan, A.N., Lee, N., Sharma, R., Kennedy, I.R., and Beckett, R. (2002) Assessment of the distribution of pesticides on soil particle fractions in simulated irrigation run-off using centrifugal SPLITT fractionation and ELISA. *Anal. Chim. Acta*, 468 (2): 199–208.
5. Fuh, C.B., Levin, S., and Giddings, J.C. (1993) Rapid diffusion coefficient measurements using analytical SPLITT fractionation: application to proteins. *Anal. Biochem.*, 208 (1): 80–87.
6. Jiang, Y., Miller, M.E., Hansen, M.E., Myers, M.N., and Williams, P.S. (1999) Fractionation and size analysis of magnetic particles using FFF and SPLITT technologies. *J. Magn. Magn. Mater.*, 194 (1–3): 53–61.
7. Keil, R.G., Tsamakis, E., Fuh, C.B., Giddings, J.C., and Hedges, J.I. (1994) Mineralogical and textural controls on the organic composition of coastal marine sediments: Hydrodynamic separation using SPLITT-fractionation. *Geochim. Cosmochim. Ac.*, 58 (2): 879–893.
8. Levin, S. and Tawil, G. (1994) Effect of surfactants on the diffusion coefficients of proteins, measured by analytical SPLITT fractionation (ASF) in the diffusion mode. *J. Pharmaceut. Biomed.*, 12 (4): 499–507.
9. Bustos, M.C. and Concha, F. (1999) Settling velocities of particulate systems 10. A numerical method for solving Kynch sedimentation processes. *Int. J. Miner. Process.*, 57 (3): 185–203.
10. Wingo, R.M., Prenger, F.C., Johnson, M.D., Waynert, J.A., Worl, L.A., and Ying, T. (2004) High gradient magnetic field split-flow thin channel (HGMF-SPLITT) fractionation of nanoscale paramagnetic particles. *Separ. Sci. Technol.*, 39 (12): 2769–2783.
11. Fuh, C.B. and Giddings, J.C. (1997) Isoelectric split-flow thin (SPLITT) fractionation of proteins. *Separ. Sci. Technol.*, 32 (18): 2945–2967.
12. Zhang, J., Williams, P.S., Myers, M.N., and Giddings, J.C. (1994) Separation of cells and cell-sized particles by continuous SPLITT fractionation using hydrodynamic lift forces. *Separ. Sci. Technol.*, 29 (18): 2493–2522.